International Journal for Modern Trends in Science and Technology
Volume 11, Issue 09, pages 248-257.
ISSN: 2455-3778 online
Available online at: http://www.ijmtst.com/vol11issue09.html
DOI: https://doi.org/10.5281/zenodo.18133873

Artificial Neural Networks (ANNs) Controller for Optimal Automatic Generation Control in Multi-Area Interconnected Power Systems

Dr. J. Srinu Naick | P. Uday Kumar | T.S. Bhanu Prakash | G.Adi Lakshmi | SK. Aisha Siddiq

Department of Electrical and Electronics Engineering, Chadalawada Ramanamma Engineering College, Andhra Pradesh, India.

To Cite this Article
Dr. J. Srinu Naick, P. Uday Kumar, T.S. Bhanu Prakash, G.Adi Lakshmi & SK. Aisha Siddiq (2025). Artificial Neural Networks (ANNs) Controller for Optimal Automatic Generation Control in Multi-Area Interconnected Power Systems. International Journal for Modern Trends in Science and Technology, 11(09), 248-257. https://doi.org/10.5281/zenodo.18133873

Article Info
Received: 02 September 2025; Accepted: 28 September 2025.; Published: 30 September 2025.

KEYWORDS

Automatic Generation Control (AGC), Artificial Neural Network (ANN), Multi-Area Interconnected Power System, Frequency Control, Area Control Error (ACE), Load Frequency Control, Renewable Energy Integration, Wind Power, Robust Control, Power System Stability.

ABSTRACT

This paper presents the design and performance evaluation of an Artificial Neural Network (ANN)–based controller for Optimal Automatic Generation Control (AGC) in multi-area interconnected power systems. Unlike conventional optimal control approaches that rely on precise mathematical models and fixed weighting matrices, the proposed ANN controller learns the nonlinear dynamics of the power system and adapts its control action in real time. The ANN is trained using system state variables such as area control error (ACE), frequency deviations, tie-line power deviations, and their integral components, enabling effective minimization of frequency and tie-line power oscillations under varying operating conditions. The proposed method is implemented on discrete two-area and multi-area interconnected power systems comprising conventional thermal units and renewable energy sources such as wind turbines. The performance of the ANN-based AGC is investigated under 1% and 5% step load perturbations (SLPs) and parameter uncertainties. Simulation results demonstrate that the proposed ANN controller significantly improves dynamic response, settling time, overshoot reduction, steady-state accuracy, and robustness when compared with existing centralized optimal quadratic AGC and other controllers reported in the literature. The obtained results confirm that the ANN-based AGC is an effective and flexible solution for modern large-scale interconnected power systems with increased penetration of renewable energy sources.

1. INTRODUCTION

The reliable operation of interconnected power systems critically depends on the continuous balance between generated power and load demand. Any sudden mismatch caused by load variations, generator outages, or renewable energy intermittency leads to deviations in system frequency and unscheduled tie-line power exchanges between interconnected areas. If not properly controlled, these deviations may degrade power quality, reduce system reliability, and, in severe cases, result in system instability or blackouts. Therefore, Automatic Generation Control (AGC), also known as Load Frequency Control (LFC), is an essential secondary control mechanism used to restore system frequency to its nominal value and maintain scheduled tie-line power flows following disturbances [1]–[3]. In traditional power systems dominated by conventional thermal and hydro generation, AGC design is commonly based on linearized system models and classical control techniques such as integral (I), proportional–integral (PI), and proportional–integral–derivative (PID) controllers [4]–[6]. Although these controllers are simple to implement, their fixed-gain structure limits performance under large load disturbances, parameter uncertainties, and nonlinear system dynamics. Moreover, tuning such controllers for multi-area interconnected systems becomes increasingly complex as system size and interconnections grow [7]. To overcome these limitations, optimal control approaches based on Linear Quadratic Regulator (LQR) theory have been widely investigated for AGC applications [8]–[10]. Centralized Optimal Quadratic AGC (COQAGC) methods formulate the AGC problem as a cost functional minimization task, where frequency deviations, tie-line power deviations, Area Control Error (ACE), and control effort are minimized simultaneously. The Functional Minimization Method (FMM) has been introduced to simplify the selection of state and control weighting matrices, providing a systematic and optimal framework for controller design [11]–[13]. While LQR/FMM-based AGC schemes offer improved transient performance and guaranteed optimality, they strongly rely on accurate mathematical modeling and fixed system parameters, which limits their robustness in practical power system environments. Modern power systems are undergoing a significant transformation due to the large-scale integration of renewable energy sources (RESs) such as wind and solar power. These sources are inherently intermittent, nonlinear, and stochastic in nature, introducing additional uncertainties into the AGC problem [14]–[16]. Furthermore, communication delays, load uncertainties, parameter variations, and nonlinear turbine–governor dynamics further challenge the effectiveness of conventional AGC strategies [17], [18]. Under such conditions, fixed-parameter optimal controllers may fail to provide satisfactory performance, motivating the need for adaptive and intelligent control techniques. In recent years, Artificial Intelligence (AI)–based methods have gained considerable attention for AGC design due to their ability to handle nonlinearities, uncertainties, and complex system dynamics without requiring precise mathematical models [19], [20]. Among these techniques, Artificial Neural Networks (ANNs) have emerged as a promising solution owing to their strong learning capability, generalization ability, and adaptability [21]. ANN-based controllers can learn the nonlinear mapping between system states and control actions directly from data, making them suitable for complex multi-area power systems with renewable energy penetration [22], [23]. Several studies have explored ANN-based AGC and LFC schemes for single-area and multi-area power systems [24]–[26]. These studies have demonstrated that ANN controllers can outperform conventional PI/PID and optimal controllers in terms of transient response, robustness, and steady-state accuracy. However, many existing ANN-based approaches are limited to continuous-time models, single-source systems, or simplified system structures. Moreover, comprehensive investigations considering discrete-time multi-area interconnected systems with renewable energy integration and comparative evaluation against centralized optimal quadratic AGC are still limited in the literature [27]–[29]. Motivated by the above research gaps, this paper proposes an ANN-based Optimal AGC framework for discrete multi-area interconnected power systems. The ANN controller is trained using key system variables such as frequency deviations, tie-line power deviations, ACE, and integral of ACE, enabling adaptive control action under varying operating conditions. The proposed approach eliminates the dependence on accurate system modeling and fixed weighting matrices, thereby enhancing robustness against step load perturbations, parameter variations, and renewable power fluctuations. The effectiveness of the proposed method is validated on discrete two-area and multi-area power systems incorporating conventional thermal units and wind energy sources. Simulation results demonstrate superior performance of the proposed ANN-based AGC compared to centralized optimal quadratic AGC and other controllers reported in the literature [30].

2. Proposed Discrete Centralized Model of AGC

In this study, a discrete centralized optimal Automatic Generation Control (AGC) scheme is developed for a two-area interconnected power system. Each control area consists of identical non-reheat thermal turbines interconnected through a tie-line. The proposed centralized closed-loop AGC structure for the two-area power system is illustrated in Fig. 1. To achieve zero steady-state error in frequency and tie-line power deviations, the integrals of Area Control Errors (ACEs) are incorporated into the system model. These Integral Area Control Errors (IACEs) act as supplementary local controllers and enhance steady-state performance.

A. Dynamics of Two-Area Interconnected Power System

The dynamics of the interconnected power system can be represented by the continuous-time state-space model as follows [27], [28]:

$$\dot{x}(t) = Ax(t) + Bu(t) + Ew(t) \quad (1)$$

$$y(t) = Cx(t) + Du(t) \quad (2)$$

Whare $x(t) \in R^{n\times 1}$ is the state vector, $u(t) \in R^{2\times 1}$ is the control input vector, and $w(t) \in R^{2\times 1}$ represents load disturbance. The matrices A, B, C, and D are of appropriate dimension

Based on the block diagram shown in Fig. 1, the first-order differential equations describing the system dynamics are given as follows [28], [29]:

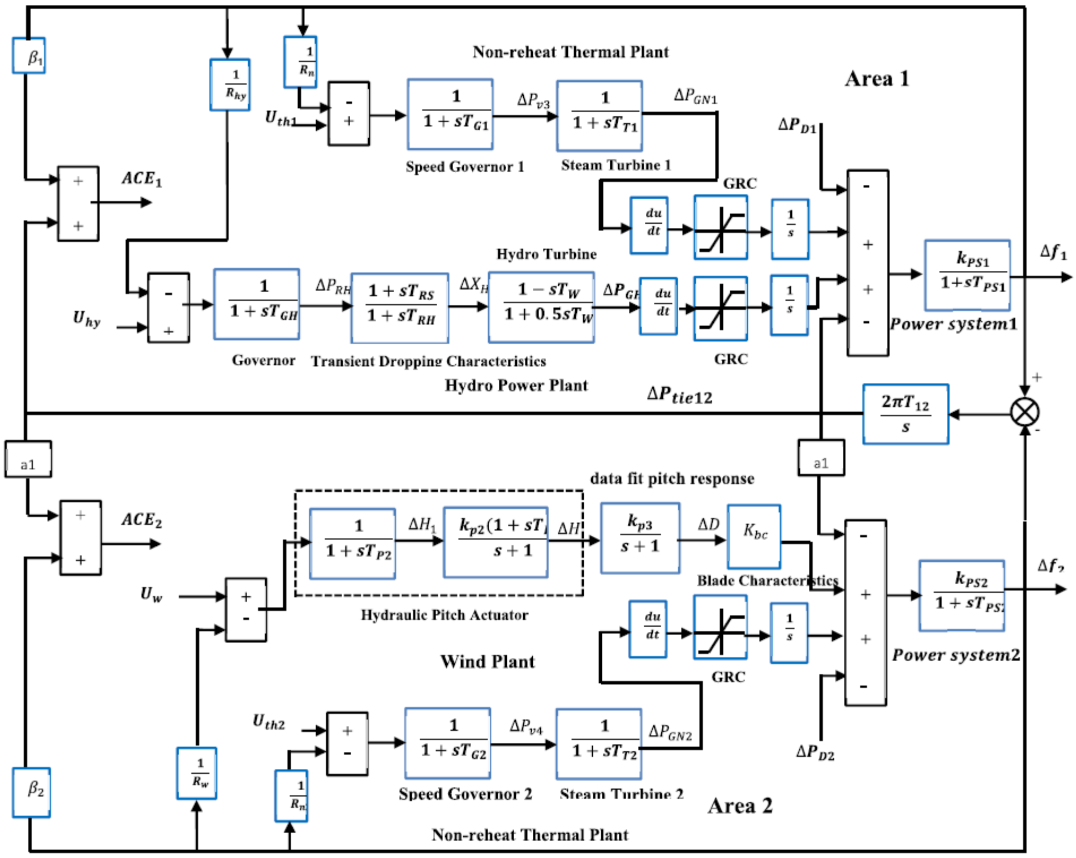

FIGURE 1. Transfer function model of multi-source power system

$$\dot{x}_1 = 2\pi T_{12} x_2 - 2\pi T_{12} x_5 \quad (3)$$

$\dot{x}_2 = -\frac{k_{ps1}}{T_{ps1}} x_1 - \frac{1}{T_{ps1}} x_2 + \frac{k_{ps1}}{T_{ps1}} x_3 - \frac{k_{ps1}}{T_{ps1}} \Delta P_{D1}$ (4)

$\dot{x}_3 = -\frac{1}{T_{T1}} x_3 + \frac{1}{T_{T1}} x_4$ (5)

$\dot{x}_4 = -\frac{1}{T_{G1}R_1} x_2 - \frac{1}{T_{G1}} x_4 + \frac{1}{T_{G1}} u_1$ (6)

$\dot{x}_5 = -\frac{a_{12}k_{ps2}}{T_{ps2}} x_1 - \frac{1}{T_{ps2}} x_5 + \frac{k_{ps2}}{T_{ps2}} x_6 - \frac{k_{ps2}}{T_{ps2}} \Delta P_{D2}$ (7)

$\dot{x}_6 = -\frac{1}{T_{T2}} x_6 + \frac{1}{T_{T2}} x_7$ (8)

$\dot{x}_7 = -\frac{1}{T_{G2}R_2} x_5 - \frac{1}{T_{G2}} x_7 + \frac{1}{T_{G2}} u_2$ (9)

$\dot{x}_8 = x_1 + \beta_1 x_2$ (10)

$\dot{x}_9 = -x_1 + \beta_2 x_5$ (11)

Where the state variables are defined as:

- $\dot{x}_1$: Tie-line power deviation between Areas 1 and 2
- $\dot{x}_2$, $\dot{x}_5$: Frequency deviation in Areas 1 and 2
- $\dot{x}_3$, $\dot{x}_6$: Turbine power output deviations
- $\dot{x}_4$, $\dot{x}_7$: Governor valve position deviations
- $\dot{x}_8$, $\dot{x}_9$: Integral of ACEs for Areas 1 and 2

The derivation of the state-space model is discussed in detail in [28], [30]. Accordingly, the state, control, disturbance, and output vectors are defined as

$x^T = [\Delta P_{tie12} \quad \Delta f_1 \quad \Delta P_{T1} \quad \Delta P_{G1} \quad \Delta f_2 \quad \Delta P_{T2} \quad \Delta P_{G2}]$
(12)

$u^T = [u_1 \quad u_2]$ (13)

$p^T = [\Delta P_{D1} \quad \Delta P_{D2}]$ 14)

$y^T = [\Delta P_{tie12} \quad \Delta f_1 \quad \Delta f_2]$ (15)

The linearized tie-line power deviation between Areas 1 and 2 is expressed as

$$\Delta P_{tie12}(s) = \frac{2\pi T_{12}}{s} (\Delta f_1 - \Delta f_2)$$

$\Delta P_{tie12}(s) = \frac{2\pi T_{12}}{s} (\Delta f_1 - \Delta f_2)$ (16)

B. Design of Discrete Centralized COQAGC

The discrete-time state-space representation of the interconnected power system is obtained from the continuous-time model using Euler's discretization method and is given by

$x(k+1) = A_k x(k) + B_k u(k) + E_k w(k)$
(17)

$x(k_0) = x_0, \quad x(k_f) = x_{k_f}$ (18)

where x(k) is the discrete-time state vector, u(k) is the control input vector, and w(k) represents load disturbances. The objective of the centralized optimal AGC problem is to determine a control law that minimizes the quadratic cost function

$J = \frac{1}{2} \sum_{k=k_0}^{\infty} [x^T(k) Q_k x(k) + u^T(k) R_k u(k)]$ (19)

subject to the discrete-time system dynamics given in (14), where Qk and Rk are the state and control weighting matrices, respectively.

The optimal feedback gain matrix is obtained by solving the steady-state discrete algebraic Riccati equation [30], [31]:

$L = [R_k + B_k^T P_k B_k]^{-1} B_k^T P_k A_k$ (20)

Where P_k satisfies

$P_k = Q_k + A_k^T [P_k - P_k B_k (B_k^T P_k B_k + R_k)^{-1} B_k^T P_k] A_k$
(21)

Substituting the optimal control law into the system model, the closed-loop discrete system is given by

$x(k+1) = [A_k - B_k (R_k + B_k^T P_k B_k)^{-1} B_k^T P_k A_k] x(k)$
(22)

The closed-loop system is stable if all eigenvalues of the closed-loop matrix lie inside the unit circle in the complex plane.

C. COQAGC Algorithm

The detailed procedure for implementing the proposed COQAGC scheme is summarized as follows:

1. Develop the continuous-time state-space model of the multi-area power system.
2. Input system parameters and operating data.
3. Augment the model by including integral of ACEs.
4. Convert the augmented model into discrete form using Euler discretization.
5. Initialize the Riccati matrix, select weighting matrices, and iteration length.
6. Compute the discrete optimal feedback gain matrix and control law.
7. Initialize state variables and simulate the closed-loop system iteratively.
8. Implement the COQAGC scheme in MATLAB/Simulink.
9. Evaluate dynamic responses under step load perturbations (SLPs).
10. Perform robustness analysis considering parameter uncertainties and generation rate constraints (GRC).

3. Problem Formulation

In a multi-area interconnected power system, variations in load demand cause imbalances between generation and consumption, leading to deviations in system frequency and unscheduled tie-line power flows. Maintaining frequency at its nominal value and regulating tie-line power exchange between control areas are the primary objectives of Automatic Generation Control (AGC). These objectives become more challenging in modern power systems due to nonlinear turbine–governor dynamics, parameter uncertainties, and the increasing integration of renewable energy sources. Consider a discrete-time multi-area interconnected power system consisting of conventional thermal units and renewable generation. For each control area, the Area Control Error (ACE) is defined as a combination of local frequency deviation and tie-line power deviation. The AGC problem aims to minimize ACE and its integral so that both frequency and tie-line power deviations are driven to zero under steady-state conditions following load disturbances. Conventional centralized AGC techniques, such as LQR/FMM-based controllers, rely on accurate system models and fixed controller parameters. However, their performance degrades under varying operating conditions and system uncertainties. To address these limitations, the AGC problem in this work is formulated as an adaptive control problem using an Artificial Neural Network (ANN). The proposed ANN-based AGC controller generates control signals based on measured system variables, including frequency deviations, tie-line power deviations, ACE, and integral of ACE. By learning the nonlinear relationship between system states and control actions, the ANN dynamically adjusts the control input to minimize frequency and tie-line power oscillations. The formulated problem seeks to ensure improved dynamic response, reduced settling time, and enhanced robustness of the interconnected power system under step load perturbations and parameter variations.

A. Design of ANN-Based AGC Controller

The Artificial Neural Network (ANN)–based controller is designed to provide adaptive control for multi-area interconnected power systems. Unlike conventional fixed-gain AGC controllers, the ANN can learn the nonlinear mapping between system states and optimal control actions, handling nonlinearities, parameter uncertainties, and renewable integration as shown in Fig.2.

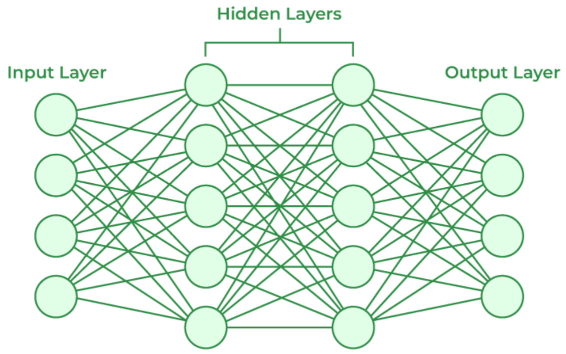

Fig.2 Implementation of ANN controller based two-area hybrid system

B. Selection of Inputs and Outputs

Let the input vector to the ANN at time step k be

$x(k) =$
$[\Delta f_1(k)\ \Delta f_2(k)\ \Delta P_{tie12}(k)\ ACE_1(k)\ ACE_2(k)\ \int ACE_1(k)\ dt\ \int ACE_2$

(23)

Where:

- $\Delta f_1(k), \Delta f_2(k)$ *are frequency deviations in Areas* 1*and*
- $\Delta P_{tie12}(k)$ *is the tie − line power deviation,*
- $ACE_1(k), ACE_2(k)$ *are Area Control Errors,*
- $\int ACE_1(k)\ dt, \int ACE_2(k)\ dtaretheintegralofACEs$

.

The **output vector** is:

$$u(k) = \begin{bmatrix} u_1(k) \\ u_2(k) \end{bmatrix} \qquad (24)$$

C. ANN Architecture

A feedforward Multilayer Perceptron (MLP) network is adopted, with one hidden layer containing nhn_hnh neurons. The output is generated as:

$$u(k) = W^{(2)}\ \phi!\left(W^{(1)}x(k) + b^{(1)}\right) + b^{(2)} \qquad (25)$$

Where:

- $\boldsymbol{W^{(1)}} \in R^{2\times n_i}$ is the weight matrix connecting inputs to hidden layer (n_i= 7 inputs),
- $\boldsymbol{b^{(1)}} \in R^{n_h}$ is the bias vector for hidden layer,
- $\phi(\cdot)$ is the **activation function** of hidden neurons, typically **tangent sigmoid:**

$$[\phi(z) = \frac{2}{1+e^{-2z}} - 1] \qquad (26)$$

- $\boldsymbol{W^{(2)}} \in R^{2\times n_h}$ is the weight matrix connecting hidden layer to output layer:
- $\boldsymbol{b^{(2)}} \in R^2$ is the bias vector for output layer.

The network maps nonlinear relationships between system states and optimal control signals.

D. Training of the ANN

The ANN is trained using supervised learning with a reference dataset (x(k),uref(k)) obtained from a conventional AGC controller (e.g., COQAGC or optimized PID). The objective is to minimize the Mean Squared Error (MSE) between ANN outputs and reference control signals:

$$E = \frac{1}{N}\sum_{k=1}^{N}||u_{\text{ref}}(k) - u(k)||^2 \quad (27)$$

The **backpropagation algorithm** is applied to update weights and biases iteratively:

$$W^{(l)}(t+1) = W^{(l)}(t) - \eta\frac{\partial E}{\partial W^{(l)}} \quad (28)$$

$$\boldsymbol{b}^{(l)}(t+1) = \boldsymbol{b}^{(l)}(t) - \eta\frac{\partial E}{\partial \boldsymbol{b}^{(l)}} \quad (29)$$

Where l=1, 2 denotes the layer index and η is the learning rate.

The **error gradient** for output neurons is computed rate:

$$\delta^{(2)} = \left(u(k) - u_{\text{ref}}(k)\right) \odot f'!\left(\text{net}^{(2)}\right) \quad (30)$$

And for hidden neurons:

$$\delta^{(1)} = \left(W^{(2)T}\delta^{(2)}\right) \odot \phi'!\left(\text{net}^{(1)}\right)$$

(31)

Where $\odot$ denotes element-wise multiplication, and $\mathbf{net}^{(1)}$, $\mathbf{net}^{(2)}$ are the net input to hidden and output layers.

D. Online Implementation

After training, the ANN controller is implemented in real-time AGC. At each sampling instant:

1. Measure the system states $x(k)$.
2. Compute the control signals:

$$u(k) = w^{(2)}\phi\left(w^{(1)}x(k) + b^{(1)}\right) + b^{(2)}$$

(33)

3. Apply $u_1(k)$ and $u_2(k)$ to the governors.
4. Repeat for each time step.

This approach allows the controller to adaptively regulate frequency and tie-line power deviations under varying operating conditions.

4. Extension to Multi-Area Multi-Source Power System

To demonstrate the effectiveness and scalability of the proposed discrete Centralized Optimal Quadratic Automatic Generation Control (COQAGC) controller, the study is extended to a multi-area multi-source interconnected power system with renewable energy sources, as shown in Fig. 3 [30]. The considered test system consists of two control areas with heterogeneous generation units. Area 1 includes a non-reheat thermal plant and a hydro power plant, while Area 2 comprises a wind power plant integrated with a non-reheat thermal plant.

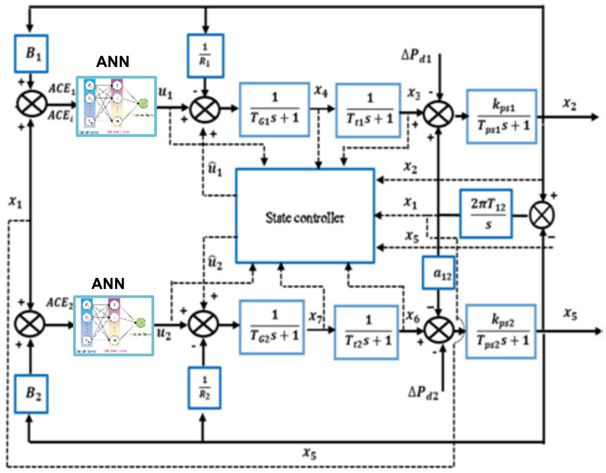

FIGURE 3. ANN Controlled Two area control closed-loop system controller.

The linearized model of the wind power plant incorporates the **pitch actuator dynamics**, a **lag compensator** to match phase and gain characteristics, and a **blade characteristics block**, as reported in [36]. The parameters of the non-reheat thermal plants are taken from Table I. The wind turbine parameters are adopted from the studies by Arya and Kumar [37] and Sahu, Griot, and Panda [34], where

TABLE 1. The parameters of the two-area thermal power system.

Parameter	Area 1	Area 2	Unit
P_R	2000	2000	MW
T_{ps}	20	20	s
T_t	0.3	0.3	s
K_{ps}	120	120	$Hz/pu, MW$
T_{12}	0.0867	0.0867	MW/Hz
T_G	0.08 sec	0.08	s
R_i	2.4	2.4	$Hz/pu, MW$
B_i	0.425	0.425	$pu\ MW/Hz$
D_i	0.0833	0.0833	N/m.s
$\Delta\delta$	30°	30°	Degree

$T_{p^1} = 6$, $T_{p^2} = 0.004$, $k_{p^2} = 1.25$, $k_{p^3} = 1.4$, $T_{g^2} = 0.08$, $k_{bc} = 0.8$, $R_w = 2.4$, and $\beta_w = 0.425$.

The hydro power plant parameters are adopted from Parmar, Majhi, and kothari, where

$T_w = 1s$, $T_{RH} = 0.3s$, $T_{RH1} = 28.75s$, $T_R = 0.11$s, $k_{r1} = 0.3$, $T_{gh} = 0.2$s, and $T_{r1} = 1$s. for both case studies, the common parameters are selected as

$k_{ps} = k_{ps1} = k_{ps2} = 120$,

$\beta_1 = \beta_2 = \beta_{hy} = \beta_w = 0.425$,

$T_{ps} = T_{ps1} = T_{ps}2 = 20$, and

$R_1 = R_2 = R_3 = R_{hy} = 2.4$.

The multi-area multi-source power system shown in Fig. 9 is modeled using **15 state variables**, defined as follows:

- $x_1 = \Delta f_1$
- $x_2 = \Delta P_{GN1}$
- $x_3 = \Delta P_{v3}$
- $x_4 = IACE_1$
- $x_5 = \Delta P_{GH}$
- $x_6 = \Delta X_H$
- $x_7 = \Delta P_{RH}$
- $x_8 = \Delta P_{tie12}$
- $x_9 = \Delta f_2$
- $x_{10} = \Delta D$
- $x_{11} = \Delta H$
- $x_{12} = \Delta H_1$
- $x_{13} = IACE_2$
- $x_{14} = \Delta P_{GN_2}$
- $x_{15} = \Delta P_{v4}$

The detailed formulation of the state vector, control input vector, disturbance vector, and the corresponding continuous-time state matrix Am, input matrix Bm, and disturbance matrix Em for the two-area multi-source power system are presented in [30]. Based on the Functional Minimization Method (FMM) described in Section III, the state and control weighting matrices Qm and Rm are constructed for the multi-area power system with renewable energy sources, following the approach in [30].

For performance comparison, the cost function proposed by Esmail and Krishnamurthy [30] is adopted and is expressed as

$$J = \frac{1}{2}\sum_{k=k_0}^{\infty}\left[B_1^2 x_1^2 + 2\beta_1 x_1 x_8 + x_8^2 + B_2^2 x_9^2 - 2\beta_2 x_9 x_8 + x_8^2 + x_4^2 + x_{13}^2 + \alpha\left(U_{th1}^2 + U_{hy}^2 + U_w^2 + U_{th2}^2\right)\right] \quad (34)$$

where α is the vector of participation factors, and Uth1, Uhy, Uw, and Uth2 represent the control signals applied to the non-reheat thermal plant in Area 1, hydro plant, wind power plant, and non-reheat thermal plant in Area 2, respectively.

The numerical values of the optimal feedback gain matrix are obtained using the discrete Riccati equation given in (16). To evaluate the dynamic performance of the multi-source interconnected power system under the proposed COQAGC controller, the following test scenarios are considered:

- Performance comparison under 1% step load perturbation (SLP) with and without Generation Rate Constraints (GRC).
- Sensitivity analysis to assess controller robustness against ±30% parameter variations.
- Performance evaluation under concurrent step load perturbations (CSLPs) applied at 5 s intervals.
- Cost function performance comparison for a 1% SLP applied in Area 1 at t=0t = 0t=0 s, while no load perturbation is applied in Area 2.

5. SIMULATION RESULTS AND DISCUSSION

The effectiveness of the proposed Artificial Neural Network (ANN)–based controller for Automatic Generation Control (AGC) is validated through extensive MATLAB/Simulink simulations on a two-area hybrid power system. To clearly highlight the improvement achieved through intelligent control, system performance is first analyzed using a conventional PI controller with fixed gains, which represents the existing control approach. Subsequently, the PI controller is replaced with the proposed ANN controller, and the dynamic responses are compared under identical operating conditions.

A. Test System and Simulation Conditions

The simulated system consists of two interconnected control areas linked by a tie-line. Area-1 comprises a photovoltaic (PV) generation unit along with local loads, while Area-2 consists of a reheat thermal power plant. The nominal system frequency is maintained at 50 Hz. The Area Control Error (ACE) of each area is used as the feedback signal for AGC operation.

To assess system dynamic performance, a step load perturbation (SLP) of 0.01 p.u. is applied in Area-1 at t=0t = 0t=0 s, while Area-2 operates under nominal load conditions. This disturbance scenario allows evaluation of frequency deviations, tie-line power exchange, and ACE responses in both areas. All simulations are carried out using the same system parameters and disturbance conditions to ensure a fair comparison between the PI and ANN controllers.

B. Performance of Conventional PID Controller (Existing Method)

Initially, the AGC system is simulated using a conventional PI controller with manually tuned gain values. The frequency deviation responses of Area-1 (Δf1) and Area-2 (Δf2) show that the PI controller is capable of restoring system frequency to its nominal value; however, the overall dynamic performance is unsatisfactory.

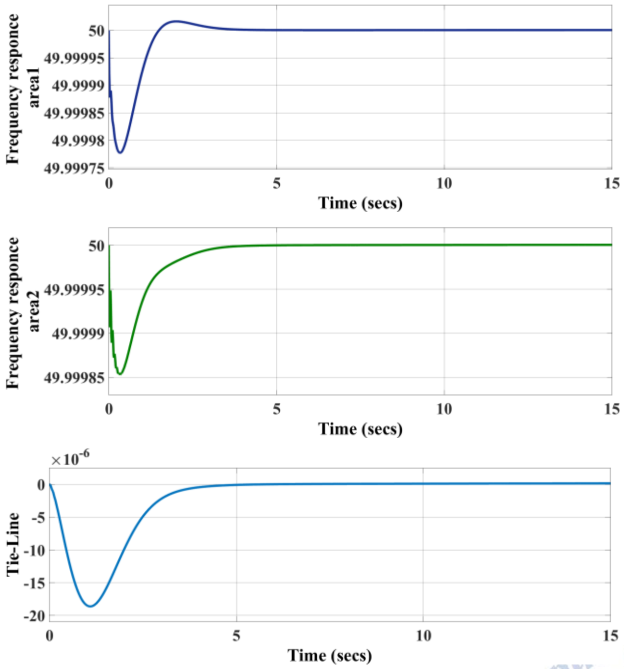

Fig.4 simulation results of PID controlled power system of two-area

Following the load disturbance, the frequency responses exhibit large initial deviations, pronounced oscillations, and a long settling time, as shown in Fig. 4. The fixed-gain nature of the PI controller limits its ability to adapt to nonlinear system dynamics and renewable power fluctuations, particularly due to the intermittent nature of PV generation in Area-1. As a result, oscillations persist for a longer duration before the system reaches steady state. Moreover, the tie-line power deviation (ΔPtie) under PI control shows sustained oscillations, indicating poor inter-area power exchange regulation. The ACE responses of both areas converge slowly to zero, demonstrating delayed correction of the generation–load imbalance. These results clearly indicate that the existing PI controller fails to provide robust AGC performance, especially in the presence of renewable energy sources and system nonlinearities.

C. Performance of Proposed ANN-Based AGC Controller

To overcome the limitations of the fixed-parameter PI controller, it is replaced with the proposed ANN-based AGC controller. The ANN generates the control signal dynamically based on real-time measurements of frequency deviation, rate of change of frequency, and ACE, thereby adapting to changing operating conditions.

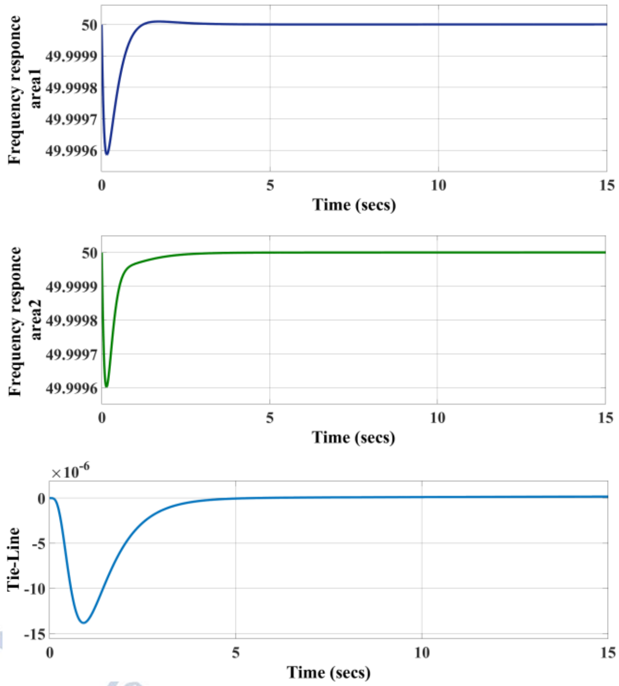

Fig.5 simulation results of ANN controlled power system of two-area

The simulation results under ANN control, shown in Fig. 5, demonstrate a significant improvement in dynamic performance. The maximum frequency deviations in both areas are considerably reduced compared to the PI controller. Oscillations are effectively suppressed, and the system reaches steady-state conditions much faster. The ANN controller exhibits strong learning and generalization capabilities, enabling it to respond efficiently to sudden load changes and PV power variations.

In addition, the tie-line power deviation settles rapidly with minimal oscillations, indicating improved coordination between the interconnected areas. The ACE signals converge quickly to zero, confirming faster restoration of power balance and enhanced AGC effectiveness. These results validate the superior adaptability and robustness of the ANN controller.

D. Comparative Performance Analysis

A quantitative comparison between the PI controller (existing method) and the ANN controller (proposed method) is carried out using standard AGC performance indices such as peak overshoot, settling time, and Integral of Time-weighted Absolute Error (ITAE). The ANN controller consistently achieves lower ITAE values, reduced overshoot, and shorter settling times compared to the PI controller, as illustrated in Fig. 6.

Further simulation studies conducted under varying load conditions confirm the robustness and consistency of the ANN-based AGC scheme. While the performance of the PI controller degrades significantly under changing operating conditions, the ANN controller maintains stable and reliable operation due to its adaptive learning nature.

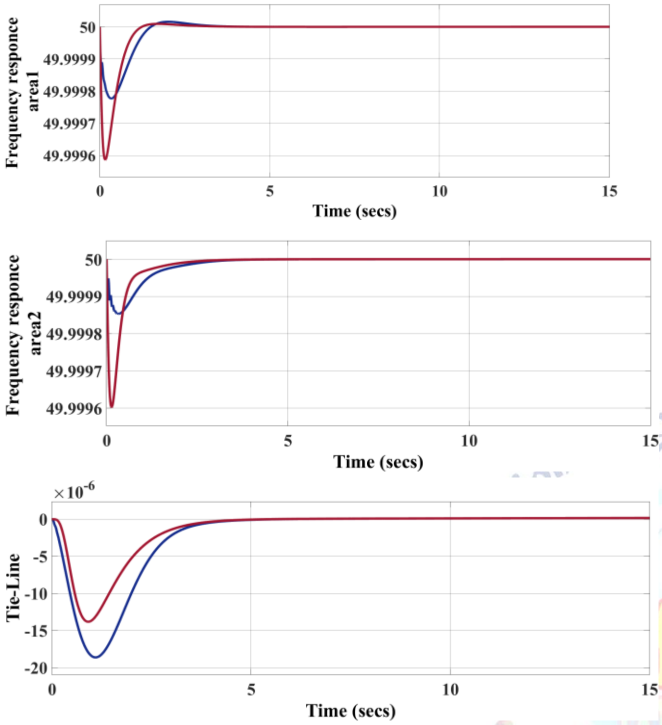

Fig. 6 Comparison of simulation results for PI and ANN controlled two-area hybrid power system

From the simulation results, it is evident that the conventional PI controller does not provide optimal AGC performance because of its fixed-gain structure, resulting in higher frequency oscillations, poor damping, and delayed settling of both frequency and tie-line power responses. In contrast, the proposed ANN-based controller significantly enhances AGC performance, offering superior damping characteristics, faster frequency recovery, and improved inter-area power regulation. Overall, the ANN-based intelligent control strategy proves to be a robust and efficient solution for AGC in hybrid PV–thermal interconnected power systems, particularly under load disturbances and renewable energy uncertainties.

6. CONCLUSION

This paper investigated the application of an Artificial Neural Network (ANN)–based controller for Automatic Generation Control (AGC) in a two-area hybrid PV–thermal interconnected power system. The performance of the proposed ANN controller was evaluated through MATLAB/Simulink simulations and compared with a conventional PI controller under identical operating conditions. Step load perturbations were applied to assess the dynamic response of system frequency, tie-line power, and Area Control Error (ACE). The simulation results indicate that the conventional PI controller, due to its fixed gain structure, is unable to provide satisfactory AGC performance in the presence of system nonlinearities and renewable energy uncertainties. Large frequency deviations, higher oscillations, and longer settling times were observed following load disturbances. In addition, tie-line power deviations and ACE responses exhibited slow convergence, which can negatively affect inter-area power exchange and overall system stability. In contrast, the proposed ANN-based AGC controller demonstrated significantly improved dynamic performance. The ANN controller effectively reduced peak frequency deviations, suppressed oscillations, and achieved faster settling of frequency and tie-line power responses. The ACE signals converged rapidly to zero, confirming improved power balance restoration and enhanced coordination between the interconnected areas. The adaptive learning capability of the ANN enabled robust performance under varying operating conditions where the conventional PI controller showed degraded behavior. Overall, the results confirm that the ANN-based AGC approach provides a robust and efficient solution for frequency regulation in hybrid interconnected power systems with renewable energy sources. The proposed controller offers superior damping characteristics, faster frequency recovery, and improved inter-area power regulation compared to conventional PI-based AGC schemes, making it a promising control strategy for modern power systems.

Conflict of interest statement

Authors declare that they do not have any conflict of interest.

REFERENCES

[1] R. Shankar, S. R. Pradhan, K. Chatterjee, and R. Mandal, "A comprehensive state of the art literature survey on LFC mechanism for power system," Renew. Sustain. Energy Rev., vol. 76, pp. 1185–1207, Sep. 2017.

[2] M. T. Alrifai, M. F. Hassan, and M. Zribi, ''Decentralized load frequency controller for a multi-area interconnected power system,'' Int. J. Electr. Power Energy Syst., vol. 33, no. 2, pp. 198–209, Feb. 2011.
[3] D. H. Tungadio, R. C. Bansal, and M. W. Siti, ''Optimal control of active power of two micro-grids interconnected with two AC tie-lines,'' Electr. Power Compon. Syst., vol. 45, no. 19, pp. 2188–2199, Nov. 2017.
[4] M. Esmail, R. Tzoneva, and S. Krishnamurthy, ''Review of automatic generation control in deregulated environment,'' IFAC-PapersOnLine, vol. 50, no. 2, pp. 88–93, Dec. 2017.
[5] W. Tan and Z. Xu, ''Robust analysis and design of load frequency controller for power systems,'' Electr. Power Syst. Res., vol. 79, no. 5, pp. 846–853, May 2009.
[6] A. Delassi, S. Arif, and L. Mokrani, ''Load frequency control problem in interconnected power systems using robust fractional PIλDcontroller,'' Ain Shams Eng. J., vol. 9, no. 1, pp. 77–88, Mar. 2018.
[7] S. R. Khuntia and S. Panda, ''Simulation study for automatic generation control of a multi-area power system by ANFIS approach,'' Appl. Soft Comput., vol. 12, no. 1, pp. 333–341, Jan. 2012.
[8] S. Prakash and S. K. Sinha, ''Simulation based neuro-fuzzy hybrid intelligent PI control approach in four-area load frequency control of interconnected power system,'' Appl. Soft Comput., vol. 23, pp. 152–164, Oct. 2014.
[9] L. Dong, Y. Zhang, and Z. Gao, ''A robust decentralized load frequency controller for interconnected power systems,'' ISA Trans., vol. 51, no. 3, pp. 410–419, May 2012.
[10] W. Chan, S. Mem, and Y. Hsu, ''Automatic generation control of interconnected power systems using variable-structure controllers,'' IEE Proc. D, Control Theory Appl., vol. 138, no. 6, pp. 579–585, 1981.
[11] Z.-Q. Wang and M. Sznaier, ''Robust control design for load frequency control using µ synthesis,'' in Proc. Conf. Rec. Southcon, Orlando, FL, USA, Mar. 1994, pp. 186–190.
[12] A. D. Falehi, ''Optimal fractional order BELBIC to ameliorate small signal stability of interconnected hybrid power system,'' Environ. Prog. Sustain. Energy, vol. 38, no. 5, pp. 1–18, Sep. 2019.
[13] A. D. Falehi, ''Robust and intelligent type-2 fuzzy fractional-order controller-based automatic generation control to enhance the damping performance of multi-machine power systems,'' IETE J. Res., vol. 68, no. 4, pp. 2548–2559, Jul. 2022.
[14] X. Shang-Guan, Y. He, C. Zhang, L. Jiang, and J. W. Spencer, ''Sampleddata based discrete and fast load frequency control for power systems with wind power,'' Appl. Energy, vol. 259, Jan. 2020, Art. no. 114202.
[15] H. Bevrani, Robust Power System Frequency Control, 2nd ed. Cham, Switzerland: Springer, 2014.
[16] K. Vrdoljak, N. Perić, and I. Petrović, ''Sliding mode based load-frequency control in power systems,'' Electr. Power Syst. Res., vol. 80, no. 5, pp. 514–527, May 2010.
[17] O. Elgerd and C. Fosha, ''Optimum megawatt-frequency control of multiarea electric energy systems,'' IEEE Trans. Power App. Syst., vol. PAS-89, no. 4, pp. 556–563, Apr. 1970.
[18] C. Fosha and O. Elgerd, ''The megawatt-frequency control problem:Anew approach via optimal control theory,'' IEEE Trans. Power App. Syst., vol. PAS-89, no. 4, pp. 563–577, Apr. 1970.
[19] A. Panwar, V. Agarwal, G. Sharma, and S. Sharma, ''Design of a novel AGC action for a linked hydro governing system,'' Electr. Power Compon. Syst., vol. 49, no. 15, pp. 1201–1211, Sep. 2021.
[20] E. Vlahakis, L. Dritsas, and G. Halikias, ''Distributed LQR design for a class of large-scale multi-area power systems,'' Energies, vol. 12, no. 14, p. 2664, Jul. 2019.
[21] Y. Arya, N. Kumar, and S. K. Gupta, ''Optimal automatic generation control of two-area power systems with energy storage units under deregulated environment,'' J. Renew. Sustain. Energy, vol. 9, no. 6, Nov. 2017, Art. no. 064105.
[22] G. Sharma, I. Nasiruddin, K. R. Niazi, and R. C. Bansal, ''Robust automatic generation control regulators for a two-area power system interconnected via AC/DC tie-lines considering new structures of matrix Q,'' IET Gener., Transmiss. Distrib., vol. 10, no. 14, pp. 3570–3579, Nov. 2016.
[23] G. Sharma, ''OptimalAGCdesign for diverse sources of power generations in each area using output vector feedback control technique,'' Int. J. Eng. Res. Afr., vol. 45, pp. 99–114, Nov. 2019.
[24] A. Prakash, P. Singh, K. Kumar, and S. K. Parida, ''Design of a reducedorder WADC for wind turbine system-integrated power system,'' IEEE Trans. Ind. Appl., vol. 58, no. 3, pp. 3250–3260, May 2022.
[25] Y. Arya, ''A new optimized fuzzy FOPI-FOPD controller for automatic generation control of electric power systems,'' J. Franklin Inst., vol. 356, no. 11, pp. 5611–5629, Jul. 2019.
[26] Y. Arya and N. Kumar, ''Fuzzy gain scheduling controllers for automatic generation control of two-area interconnected electrical power systems,'' Electr. Power Compon. Syst., vol. 44, no. 7, pp. 737–751, Apr. 2016.
[27] D. Das, S. K. Aditya, and D. P. Kothari, ''Dynamics of diesel and wind turbine generators on an isolated power system,'' Int. J. Electr. Power Energy Syst., vol. 21, no. 3, pp. 183–189, Mar. 1999.
[28] Y. Arya and N. Kumar, ''AGC of a multi-area multi-source hydrothermal power system interconnected via AC/DC parallel links under deregulated environment,'' Int. J. Electr. Power Energy Syst., vol. 75, pp. 127–138, Feb. 2016.
[29] K. P. S. Parmar, S. Majhi, and D. P. Kothari, ''Load frequency control of a realistic power system with multi-source power generation,'' Int. J. Electr. Power Energy Syst., vol. 42, no. 1, pp. 426–433, Nov. 2012.
[30] S. Gouran-Orimi and A. Ghasemi-Marzbali, ''Load frequency control of multi-area multi-source system with nonlinear structures using modified grasshopper optimization algorithm,'' Appl. Soft Comput., vol. 137, Apr. 2023, Art. no. 110135.